

LiNbO₃:Tm³⁺ Crystal: Material for Radiation-Balanced Laser in the Wavelength Range of 1650 – 2000 nm

N. Mkhitarian¹, G. Demirkhanyan^{1,2}, N. Kokanyan^{3,4}, E. Kokanyan^{1,2}

¹Armenian State Pedagogical University after Kh. Abovyan, Yerevan, Armenia

²Institute of Physical Research, National Academy of Sciences of Armenia, Ashtarak, Armenia

³Chaire Photonique, Laboratoire Matériaux Optiques Photonique et Systèmes Centrale Supélec (LMOPS), France

⁴Lorraine University, LMOPS, Metz, France

E-mail: edvardkokanyan@gmail.com

(Received: November 10, 2023; Revised: November 21, 2023; Accepted: November 25, 2023)

Abstract. The absorption and emission cross-section spectra of *LiNbO₃:Tm³⁺* crystals were investigated within the wavelength range of 1650 – 2000 nm at room temperature. This study delves into the potential for achieving radiation-balanced lasing. Optimal parameters for both the pump and emission wavelengths, denoted as $\lambda_{OP} = 1837$ nm and $\lambda_{OL} = 1852$ nm, respectively, were determined. At these wavelengths, the corresponding optimal values for gain $F_{gain} \cong 0.8 \times 10^{-22}$ cm² and radiation-balanced generation efficiency $F_{eff} \cong 0.4 \times 10^{-22}$ cm² were identified. These findings underscore the feasibility of radiation-balanced lasing in *LiNbO₃:Tm³⁺* crystals under the specified conditions.

Keywords: Lithium niobate, crystal, optical cooling, balanced laser

DOI: 10.54503/18291171-2023.16.3-102

1. Introduction

The inception of a self-cooling solid-state laser, specifically a radiation-balanced laser, utilizing doped rare-earth (RE) ions was initially proposed in [1]. The fundamental principle underlying the functionality of a radiation-balanced (RB) laser rests on the prospect of fully or partially offsetting the heat generated through stimulated emission by leveraging cooling through anti-Stokes fluorescence within the active medium. Consequently, the operation of such lasers is designed to minimize, if not eliminate, internal heat generation. A comprehensive exploration of the operational mechanisms of solid-state RB lasers can be found in [2–5]. The experimental realization of the first bulk radiation-balanced (RB) laser in a *KGd(WO₄)₂:Yb³⁺* crystal is documented in [6].

Numerous theoretical and experimental investigations are dedicated to exploring new solid-state materials doped with RE ions, exhibiting the requisite spectroscopic properties for achieving radiation-balanced (RB) generation, as extensively documented in [3, 7-9]. In [3], the potential for creating RB lasers based on *KY(WO₄)₂:Yb* crystals was thoroughly examined. [8] delved into RB lasers based on Yb-doped ZBLANP glass, while [9] focused on RB lasers using *YAG:Yb³⁺* ceramics. It is noteworthy that *KY(WO₄)₂:Yb* crystal stands out among Yb-doped materials for its ability to achieve RB generation in the wavelength range of 1050 – 1070 nm (refer to Table 3). Simultaneously, it is evident that this observation does not diminish the ongoing exploration for solid materials doped with RE ions, especially for RB generation in different wavelength regions. For instance, in [10], the study investigated the RB generation potential of a *LiNbO₃:Er³⁺* crystal in the 1.5 μm region.

This article assesses the suitability of the *LiNbO₃:Tm³⁺* (*LN:Tm*) crystal as a material for an RB laser, contributing to the broader understanding of materials suitable for achieving radiation balance in laser systems.

2. Parameters of RB generation

As is well-established, a prerequisite for the optical cooling effect and the feasibility of achieving radiation-balanced (RB) generation is expressed by equation (1):

$$\lambda_F < \lambda_p < \lambda_L \quad (1)$$

Here, λ_p and λ_L denote the pump and luminescence wavelengths, respectively, while λ_F represents the average luminescence wavelength determined by the expression:

$$\lambda_F = \frac{\int \lambda I_L(\lambda) d\lambda}{\int I_L(\lambda) d\lambda}, \quad (2)$$

where $I_L(\lambda)$ is the luminescence intensity.

The efficiency of optical cooling is quantified by the expression [1, 3]:

$$F_{cool} \equiv \frac{\eta_c(\lambda_p)}{N_t} = \sigma_{abs}(\lambda_p) \left[\frac{\lambda_p}{\lambda_F} - 1 \right], \quad (3)$$

where N_t is the concentration of active ions, and $\sigma_{abs}(\lambda_p)$ is the absorption cross-section at the pump wavelength.

To achieve a state of radiation balance, it is imperative that the absorbed and emitted power densities coincide at each point within the mode volume, satisfying condition (1). Simultaneously, when the quantum yield of fluorescence approaches unity, the stability of the radiation balance state is contingent on the pump intensity I_p and lasing intensity I_L , satisfying:

$$\frac{I_L}{I_{Lsat}} = \left[1 - \frac{\beta(\lambda_L)}{\beta(\lambda_p)} \left(1 + \frac{I_{Psat}}{I_p} \right) \right]^{-1}, \quad (4)$$

where I_{Psat} and I_{Lsat} are the corresponding saturation intensities, defined as:

$$I_{Psat} = \frac{hc}{\lambda_F \tau \sigma_{abs}(\lambda_p)} \times \frac{\lambda_L - \lambda_F}{\lambda_L - \lambda_p} \beta(\lambda_p), \quad I_{Lsat} = \frac{hc}{\lambda_F \tau \sigma_{abs}(\lambda_L)} \times \frac{\lambda_p - \lambda_F}{\lambda_L - \lambda_p} \beta(\lambda_L) \quad (5)$$

Here, τ is the spontaneous lifetime of the excited level of the active ion, h is the Planck constant, c is the speed of light, and the coefficient $\beta(\lambda)$ is determined by the expression:

$$\beta(\lambda) = \frac{\sigma_{abs}(\lambda)}{\sigma_{abs}(\lambda) + \sigma_{em}(\lambda)} \quad (6)$$

Under high pump intensities ($I_p \gg I_{Psat}$), equation (4) yields the minimum value of laser radiation intensity:

$$I_{Lmin} = \frac{\beta(\lambda_p)}{\beta(\lambda_p) - \beta(\lambda_L)} I_{Lsat} \quad (7)$$

Similarly, at high intensities of laser radiation ($I_L \gg I_{Lsat}$), for the minimum value of pump intensity, we obtain:

$$I_{Pmin} = \frac{\beta(\lambda_L)}{\beta(\lambda_p) - \beta(\lambda_L)} I_{Psat} \quad (8)$$

The efficiency of RB generation is articulated by the expression:

$$\frac{\eta(\lambda_P, \lambda_L, I_P)}{N_t} \equiv \frac{1}{N_t I_P} \frac{\partial I_L}{\partial z} = \sigma_{abs}(\lambda_P) \eta_0 \frac{\beta(\lambda_P) - \beta(\lambda_L)}{\beta(\lambda_P)} \quad (9)$$

where in (9), $\eta_0 = \frac{\lambda_P - \lambda_F}{\lambda_L - \lambda_F}$ is the so-called internal optical efficiency of RB generation.

The maximum gain coefficient $\eta_0 = \frac{\lambda_P - \lambda_F}{\lambda_L - \lambda_F}$ corresponding to the operation of an RB laser at high pump intensities has the following form [1]:

$$\frac{g_{max}}{N_t} = \sigma_{abs}(\lambda_L) \frac{\beta(\lambda_P) - \beta(\lambda_L)}{\beta(\lambda_L)} \quad (10)$$

It is pertinent to note that when examining specific crystalline systems, multiple pump channels and corresponding emission channels may satisfy condition (1). In such cases, the optimal values of gain and RB generation efficiency are determined by selecting the optimal pump wavelengths λ_{OP} , and lasing wavelengths λ_{OL} from the condition of achieving the maximum product $g_{max} \times \eta$ [1, 3].

3. Possibilities of LN:Tm crystal for RB generation

The spectroscopic characteristics of the *LN:Tm* crystal within the wavelength range of 1650 – 1970 nm were investigated in previous studies [10–12]. These investigations involved the construction of wave functions for the Stark levels within the ground ³H₆ and the first excited ³F₄ multiplets, elucidating key spectroscopic features. Furthermore, an exhaustive exploration of the *LN:Tm* crystal's potential as a fundamental component in optical cooling systems has been undertaken [13].

Fig.1 presents the luminescence intensity spectra of *LN:Tm* within the 1650 – 2000 nm range, excited at a wavelength of 800 nm, alongside the corresponding transmission spectrum. The average luminescence wavelength (λ_f) was calculated using formula (2) and found to be $\lambda_f = 1818.6$ nm. The absorption coefficient denoted as $k(\lambda)$ was derived from the transmission spectrum using the expression $k(\lambda) = \frac{1}{d} \ln \left(\frac{I_0}{I} \right)$ where "d" represents the length of the crystal. Subsequently, the absorption cross section $\sigma_{abs}(\lambda)$ was determined as $\sigma_{abs}(\lambda) = \frac{k(\lambda)}{N_{Tm}}$ with N_{Tm} being the concentration of Tm ions in the crystal, equal to $2 \times 10^{20} \text{ cm}^{-3}$.

Utilizing the radiation spectrum depicted in Fig.1(a), we determined the radiation cross section employing the Fuechtbauer-Ladenburg formula:

$$\sigma_{em} = \frac{\lambda^5}{8\pi c n^2 \tau_{rad}} \frac{I_{em}(\lambda)}{\int \lambda I_{em}(\lambda) d\lambda} \quad (11)$$

Here, "c" represents the speed of light, "n" is the refractive index (set to 2.2), and τ_{rad} denotes the radiative lifetime of the excited multiplet, specifically measured as 1.05 ms.

Fig.2a and 2b show case the absorption and emission cross section spectra at room temperature. The analysis of these figures, and particularly Fig.2b and Fig.3, highlights that absorption and emission become prominent at specific wavelengths: 1820, 1822, 1826, 1829, 1837, 1847, 1852, 1854, 1863,

1865, 1883, 1892, 1908, 1918, 1938, 1948, and 1967 nm, aligning with the conditions stipulated in equation (1).

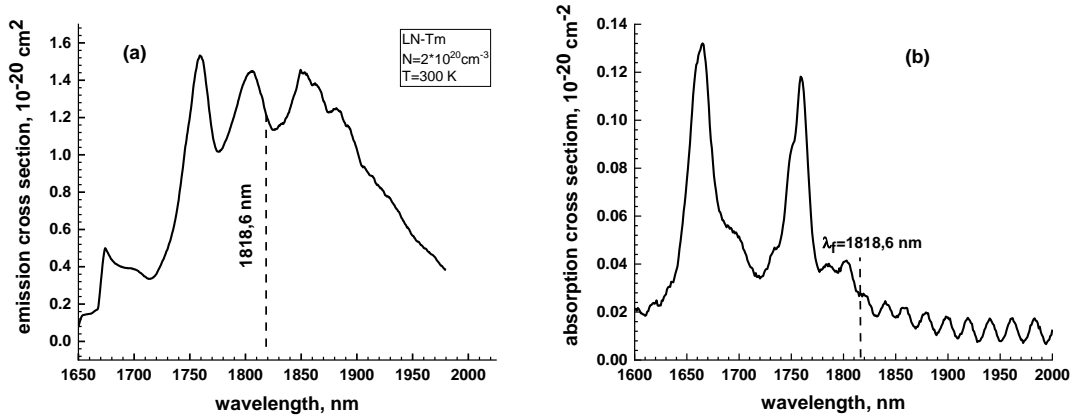


Fig. 1. (a) Emission intensity; (b) transmission intensity.

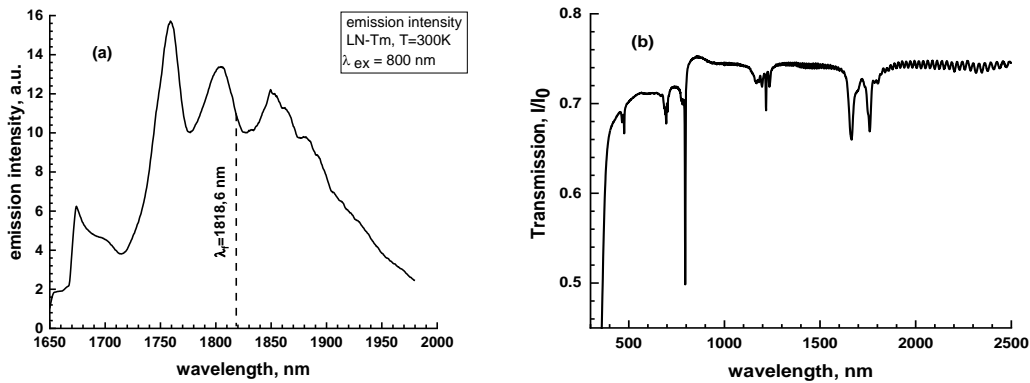


Fig. 2. Cross section of (a) emission, (b) absorption.

Table 1 presents cross-sectional values obtained from absorption and emission spectra at specified wavelengths. Excitation wavelengths, paired with their corresponding luminescence wavelengths while adhering to condition (1), are grouped in Table 2. The calculated parameters for RB generation, employing formulas (3) – (10), are also included, yielding an efficiency of at least 10^{-23} cm^2 .

Table 2 reveals that the maximum gain value, g_{max} , is achieved when the pump wavelength is $\lambda_{OP} = 1837 \text{ nm}$ (transition $\nu_7 \rightarrow \mu_3$) and generation occurs at the wavelength $\lambda_{OL} = 1852 \text{ nm}$ (transition $\mu_4 \rightarrow \nu_9$).

The optimal values for gain, $F_{gain} = g_{max}(\lambda_{OP}, \lambda_{OL})/N_t$ and efficiency, $F_{eff} \equiv \eta_L \frac{(\lambda_{OP}, \lambda_{OL})}{N_t}$, are approximately $F_{gain} \cong 0.83 \times 10^{-22} \text{ cm}^2$ and $F_{eff} \cong 0.38 \times 10^{-22} \text{ cm}^2$. Notably, when excited at a wavelength of 1837 nm , the optical cooling efficiency reaches its maximum value $F_{cool} = 0.144 \times 10^{-22} \text{ cm}^2$.

For comparative analysis, Table 3 presents the parameter values associated with the radiation generation of materials doped with rare earth ions. Notably, the $KY(WO_4)_2:Yb^{3+}$ crystal maintains an unequivocal leadership, exhibiting optical cooling efficiency and RB generation at $\lambda_{OL} = 1041 \text{ nm}$ that surpasses other materials by an order of magnitude.

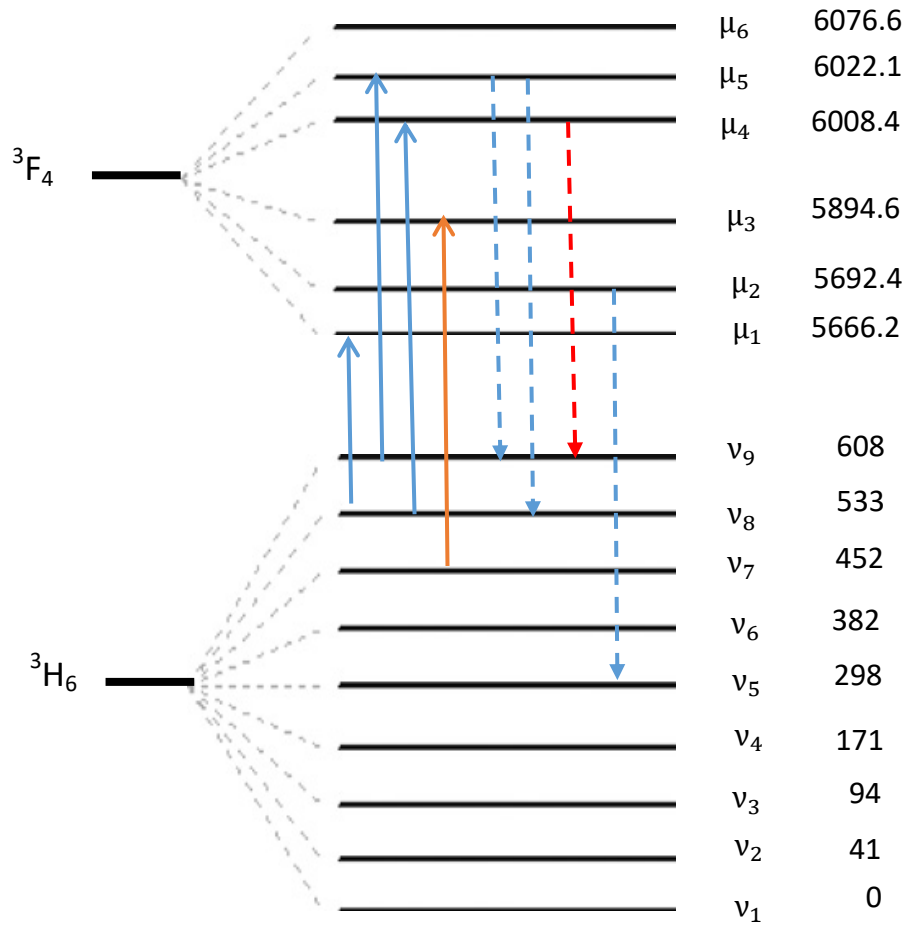


Fig. 3. Diagram of the Stark levels of the ground and first excited levels multiplets of the Tm^{3+} ion in LN [13]. The energy levels are given in cm^{-1} .

Table 1. Absorption and emission cross sections at wavelengths λ_p and λ_L

λ_p , nm	$\sigma_{abs}(\lambda_p)$, $10^{-20} cm^2$	$\sigma_{em}(\lambda_p)$, $10^{-20} cm^2$	λ_L , nm	$\sigma_{abs}(\lambda_L)$, $10^{-20} cm^2$	$\sigma_{em}(\lambda_L)$, $10^{-20} cm^2$
1820	0.0272	1.1923	1822	0.0266	1.160
1822	0.0266	1.1603	1826	0.0227	1.137
1826	0.0227	1.1368	1829	0.0188	1.151
1829	0.0188	1.1453	1837	0.0219	1.201
1837	0.0219	1.2008	1847	0.0187	1.391
1847	0.0187	1.3913	1852	0.0178	1.439
1852	0.0178	1.4391	1854	0.0192	1.433
1854	0.0192	1.4329	1863	0.0189	1.375
1863	0.0189	1.3752	1865	0.0157	1.365
1865	0.0158	1.3651	1883	0.0163	1.241
1883	0.0163	1.2411	1892	0.0125	1.156
1892	0.0125	1.1556	1908	0.0098	0.923
1908	0.0098	0.9234	1918	0.0168	0.838
1918	0.0168	0.8378	1938	0.0156	0.692
1938	0.0156	0.6921	1948	0.0093	0.587
1948	0.0093	0.5878	1967	0.0120	0.466
1967	0.0120	0.4662	1977	0.0109	0.399

Table 2. Parameters of RB generation of $LN:Tm^{3+}$ crystal.

λ_p nm	F_{cool} , $10^{-22}cm^2$	λ_L , nm	η_0 , %	$I_{P_{min}}$	$I_{L_{min}}$	$\frac{\eta}{N_t}$	$\frac{g_{max}}{N_t}$	$\frac{\eta}{N_t} \times \frac{g_{max}}{N_t}$
				$\frac{kW}{cm^2}$		$10^{-22}cm^2$		$10^{-44}cm^4$
1822 $\nu_8 \rightarrow \mu_5$	0.005	1829($\mu_5 \rightarrow \nu_9$)	32.7	30.8	14.6	0.252	0.742	0.19
		1847($\mu_5 \rightarrow \nu_8$)	12.0	13.5	2.3	0.133	1.289	0.17
		1852($\mu_4 \rightarrow \nu_9$)	10.2	10.9	2.1	0.126	1.485	0.19
		1854($\mu_2 \rightarrow \nu_5$)	9.6	13.0	1.8	0.107	1.335	0.14
1826 $\nu_9 \rightarrow \mu_5$	0.009	1829($\mu_5 \rightarrow \nu_9$)	71.2	136.0	116.9	0.289	0.410	0.12
		1847($\mu_5 \rightarrow \nu_8$)	26.1	24.3	7.7	0.191	0.890	0.17
		1852($\mu_4 \rightarrow \nu_9$)	22.2	18.3	5.2	0.189	1.072	0.20
		1854($\mu_2 \rightarrow \nu_5$)	20.9	22.5	5.6	0.154	0.923	0.14
1837 $\nu_7 \rightarrow \mu_3$	0.144	1847($\mu_5 \rightarrow \nu_8$)	64.8	65.8	7.0	0.368	0.655	0.24
		1852($\mu_4 \rightarrow \nu_9$)	55.1	38.8	26.3	0.383	0.829	0.32
		1854($\mu_2 \rightarrow \nu_5$)	52.0	47.7	28.3	0.298	0.681	0.20
1938 $\nu_8 \rightarrow \mu_2$	0.102	1948($\mu_1 \rightarrow \nu_8$)	92.3	439.1	679.7	0.421	0.384	0.16

Table 3. Parameters of optimal RB generation of RE^{3+} doped materials.

Matrix	referen ces	λ_F	λ_{op}	λ_{OL}	η_o	τ	$I_{P_{min}}$	$I_{L_{min}}$	F_{cool}	F_{eff}	F_{gain}
		nm			%	ms	$\frac{kW}{cm^2}$		$10^{-22}cm^2$		
$LN:Tm$	Current paper	1818.6	1837	1852	55	1.1	38.8	26.3	0.14	0.4	0.8
$LN:Er$	[10]	1543	1545	1559.5	87	7	1.3	2.1	0.06	1.7	11.7
$YAG:Ybceramics$	[9]	1018	1030	1050	39	0.9	5.9	53.3	0.14	3.3	1.3
$LuAG:Yb$	[2]	1002	1033	1048	67	0.9	26	303	0.49	5.1	0.8
$KY(WO_4)_2:Yb$	[3]	992	1002	1041	20	0.6	1.6	5.5	1.50	41	36
$ZBLANP:Yb$	[8]	995	1005	1024	36	1.7	38	46	0.07	1.3	2.4
$Rb_2NaYF_6:Yb$	[4]	996	1011	1068	20	10.8	1.8	17	0.02	0.25	0.34

4. Conclusions

Drawing upon the absorption and emission spectra, we identified the parameters governing the optimal RB generation of the $LN:Tm$ crystal, specifically at a wavelength of 1852 nm with pumping at 1837 nm. The observed relatively modest values of efficiency ($F_{eff} = 0.8 \times 10^{-22}cm^2$) and gain ($F_{gain} = 0.81 \times 10^{-22}cm^2$) stem from the diminished absorption levels within the wavelength range of 1600 – 2000 nm. Notably, despite these lower values, the $LN:Tm$ crystal demonstrates a commendable cooling efficiency coefficient, rendering it a strong contender against $LN:Er$, $ZBLANP:Yb$ and $Rb_2NaYF_6:Yb$ for application in optical cooling systems. Additionally, it competes favorably with the $Rb_2NaYF_6:Yb$ crystal for RB generation.

References

- [1] S.R. Bowman, IEEE J. Quantum Electron. **35** (1999) 115.
- [2] C.E. Mungan, T.R. Gosnell, Adv. At. Mol. Opt. Phys. **40** (1999) 161.
- [3] S.R. Bowman, C.E. Mungan, Trends in Optics and Photonics **34** (2000) 446.
- [4] G. Nemova, R. Kashyap, Rep. Prog. Phys. **73** (2010) 086501.

- [5] G. Nemova, Appl. Sci. **11** (2021) 7539.
- [6] S.R Bowman, N.W. Jenkins, B. Feldman, S. O'Connor, Proc. Conf. Lasers and Electro-Optics (Long Beach, CA, USA 2002).
- [7] S.R. Bowman, S. O'Connor, S. Biswal, IEEE J. Quantum Electron. **41** (2005) 1510.
- [8] C.W. Hoyt, M. Sheik-Bahae, R.I. Epstein, B.C. Edwards, J.E. Anderson, Phys. Rev. Lett. **85** (2000) 3600.
- [9] G. Demirkhanyan, B. Patrizi, R. Kostanyan, G. Toci, M. Vannini, A. Pirri, J. Li, Y. Feng, D. Zargaryan, J. Cont. Phys. (Arm. Acad. Sci.) **57** (2022) 123.
- [10] J.O. Tocho, L. Nunez, J.A. Sanz-Garsia, A.F. Cusso, D.C. Hanna, A.C. Tropper, S.J. Field, D.P. Shepnd, A.C. Large, J, de Physique, Colloque C7, supplement au J. de Physique III, **1** (1991) 293.
- [11] P.X. Zhang, J.G. Yin, R. Zhang, H.Q. Li, J.Q. Xu, Y. Hang, Las. Phys. **24** (2014) 035805.
- [12] E. Kokanyan, G. Demirkhanyan, H. Demirkhanyan. J. Cont. Phys. (Arm. Acad. Sci.) **53** (2018) 227.
- [13] N. Kokanyan, N. Mkhitaryan, G. Demirkhanyan, A. Kumar, M. Aillerie, D. Sardar, E. Kokanyan, Crystals **11** (2021) 50.